Study of the Antibacterial Behavior of Wire Arc Sprayed Copper Coatings

O. Sharifahmadian, H. R. Salimijazi, M. H. Fathi, J. Mostaghimi & L. Pershin

Journal of Thermal Spray Technology

ISSN 1059-9630
Volume 22
Combined 2-3

J Therm Spray Tech (2013) 22:371-379
DOI 10.1007/s11666-012-9842-2

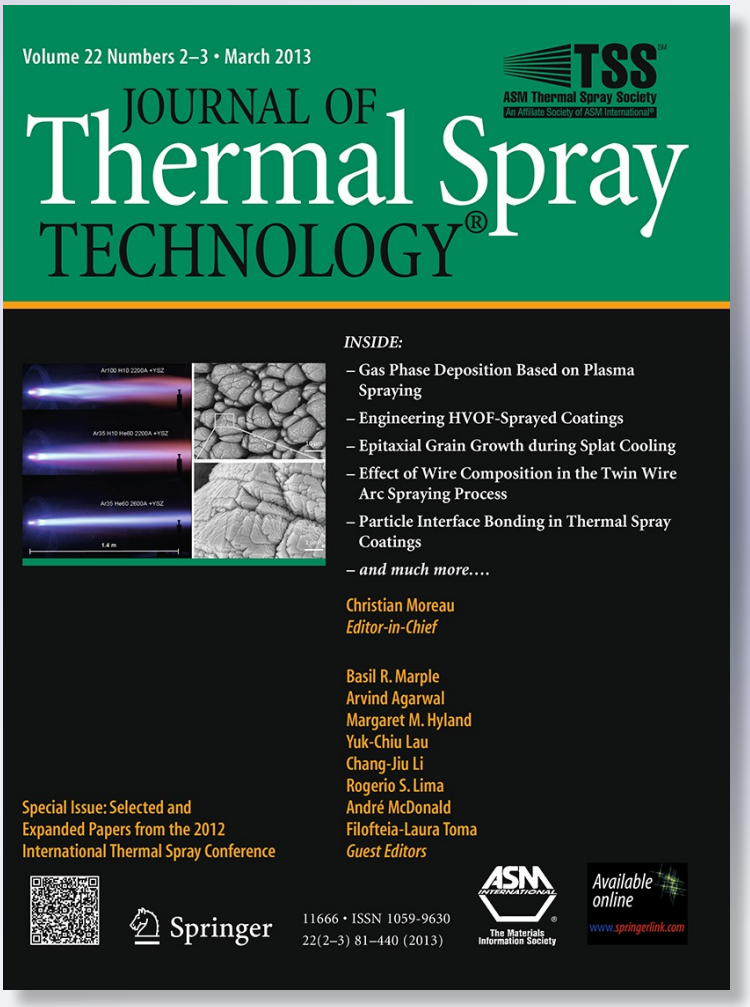

Springer

JTTEE5 22:371–379
DOI: 10.1007/s11666-012-9842-2
1059-9630/$19.00 © ASM International

Study of the Antibacterial Behavior of Wire Arc Sprayed Copper Coatings

O. Sharifahmadian, H.R. Salimijazi, M.H. Fathi, J. Mostaghimi, and L. Pershin

(Submitted June 18, 2012; in revised form October 7, 2012)

Antibacterial surfaces such as silver and copper coated areas reduce risk of bacterial growth considerably. In this study, wire arc spraying has been utilized to produce an antibacterial copper coating with ultrafine microstructure on stainless steel substrate. The chemical composition, microstructure, and surface morphology of copper coatings were characterized with x-ray diffraction and scanning electron microscope. Determination of thickness and adhesion of the coating were investigated. The antibacterial property of copper coatings was analyzed by both gram negative *Escherichia coli* NCTC 10418 and gram positive *Staphylococcus aureus* NCTC 11047. The antibacterial performance of coatings was compared to that of stainless steel 316 and a micrograin structure of the commercially available copper. Results indicated that the as-sprayed copper coatings have excellent antibacterial behavior compared to stainless steel and micrograin copper, which can be attributed to the presence of the ultrafine grain size, micropores, and crystallographic defects in the microstructure.

Keywords antibacterial, coating, copper, grain size, ultrafine structure, wire arc spray

1. Introduction

In the modern life with scientific and technological advances, considerable attention is paid to the safety, sanitation, and health of environments. Therefore, daily appliances are increasingly being designed with antibacterial features (Ref 1). Bacterial infection is one of the major clinical complications. Prevention of bacterial-related infection remains a major challenge for the delivery of quality medical care, and the problem results in a high rate of mortality and morbidity resulting in increasing health care costs significantly (Ref 2-4).

Silver and copper have been widely utilized as effective materials for sterilizing liquids and human tissues for centuries. Some advantages of copper materials, including their bactericidal activity, were well known even since the time of ancient civilizations (Ref 5). Today, copper sometimes is utilized as an agent for purification of water and inactivation of some microorganisms and bacteria (Ref 6). In spite of the negligible responsiveness of human tissues to copper, microorganisms show high sensitivity to copper (Ref 7, 8). Recently, due to the development of some drug-resistant bacteria strains, the antibacterial activity of nanostructures or ultrafine grain materials such as silver and copper has received great attention (Ref 9, 10). For instance, silver nanoparticles and nanostructures with a high bactericidal activity have been widely applied in medicine to inhibit colonization by the bacteria on prostheses, dental materials, and wound dressing, and to reduce infections in burn treatments (Ref 11-13). Antibacterial activity of copper nanostructures and ultrafine grains has not been studied due to fast oxidation of metallic copper and both chemical and physical instability of the copper oxides formed at temperature below 200 °C, particularly if Cu^{2+} are formed (Ref 14, 15).

Copper could inhibit the function of respiratory enzymes near the cell membranes by binding to their thiol groups. Copper ions could also participate in some chemical reactions. These reaction mechanisms involve copper oxide (CuO) to produce the reactive species required for the cell destruction. The reactive oxide species, such as the hydroxide ion and hydroxyl radical, play a key role in chemically attacking and damaging the cell wall. As a result, cellular integrity will be compromised by, first, OH radicals attacking the peptidoglycan layer in the cell wall that protects the bacteria. That starts the chain of polymerization reactions, damaging the cell wall and finally killing the bacteria (Ref 16, 17).

Many studies have been focused on the use of thermal spraying to produce antibacterial coatings. For example, thermal-sprayed nanostructured TiO_2 coatings exhibited photocatalytic bactericidal activity with *P. aeruginosa*

This article is an invited paper selected from presentations at the 2012 International Thermal Spray Conference and has been expanded from the original presentation. It is simultaneously published in *Thermal Spray 2012: Proceedings of the International Thermal Spray Conference, Air, Land, Water, and the Human Body: Thermal Spray Science and Applications,* Houston, Texas, USA, May 21-24, 2012, Basil R. Marple, Arvind Agarwal, Laura Filofteia-Toma, Margaret M. Hyland, Yuk-Chiu Lau, Chang-Jiu Li, Rogerio S. Lima, and André McDonald, Ed., ASM International, Materials Park, OH, 2012.

O. Sharifahmadian, H.R. Salimijazi, and **M.H. Fathi**, Department of Materials Engineering, Isfahan University of Technology, Isfahan 84156-83111, Iran; and **J. Mostaghimi** and **L. Pershin**, Department of Mechanical & Industrial Engineering, University of Toronto, Toronto, ON Canada. Contact e-mail: jazi@mie.utoronto.ca.

Table 1 Wire arc spray parameters

Gun	Value arc
Feed rate	82 g/min
Spray distance	100 mm
Current	200 A
Voltage	33 V

(Ref 18). Work by George et al. and McDonald et al. has shown that using flame spraying and HVOF is possible to fabricate nanostructured titania-copper composite coatings that combine the photocatalytic activity of TiO_2 and the bactericidal properties of copper (Ref 17, 18). Highly bioactive silver and silver/titania composite films grown by chemical vapor deposition exhibited a certain degree of self-cleaning capability. TiO_2 layers fabricated by pulsed laser deposition followed by thermal treatment illustrated high photocatalytic efficiency in the degradation of stearic acid (Ref 19, 20).

Determining an appropriate copper coating deposition technique to produce coatings with high antibacterial properties is essential (Ref 12). Twin wire arc spray is well known as one of the less expensive thermal spraying processes with an ability to produce dense coatings with a high deposition rate (Ref 21). The data from this preliminary investigation indicated that there are better surfaces than stainless steel that can be applied for antibacterial applications. Stainless steel has often been selected as the most common material because of its looks and because it can easily be cleaned. However, as it shown in studies (Ref 22, 23), *E. coli* O157 can survive for extended periods of time on the stainless steel surface indicating that a potential contamination risk could occur if a surface was not adequately cleaned. It was proven that the microstructure of these coatings mainly depends on the spray parameters. In the presented work, the wire arc spraying technique was used to deposit copper coatings on stainless steel substrates. The microstructure and antibacterial properties of the coatings were characterized and investigated comprehensively.

2. Materials and Methods

2.1 Materials and Preparation

In the current study, the wire arc spraying technique was utilized to deposit copper coating on stainless steel 316 substrates. Two consumable copper wires (99.9%) with a 1.6-mm diameter (Metco Copper, Sulzer Metco, Westbury, NY, USA) were fed into the wire arc spray gun (VALUARC 300, also from Sulzer Metco). The gun was used with a high velocity converging nozzle. The wire arc spray process parameters are tabulated in Table 1.

Commercially available copper anode sheet with 99.99% purity according to ASTM-B115 standard was used for comparison studies. Stainless steel 316 also was utilized as a reference. All samples were cut into 10×10 mm^2 pieces with 1 mm thickness.

2.2 Characterization of Surfaces

The phase composition of the coating surface was analyzed using a X-pert Philips XRD instrument with Cu Kα ($\lambda = 1.542$ nm) radiation. The XRD patterns were recorded in the 2θ range of 20°-80° (step size: 0.05° and time per step: 1 s).

An etchant (1.50 mL HNO_3, 0.5 g $AgNO_3$, and 50 mL H_2O) was used to reveal the microstructure of the copper coating and commercial copper anode (Ref 24). Microstructural observations by scanning electron microscopy (SEM, Philips XL 30) were performed on the polished sample cross sections for the coating thickness and porosity evaluation. Energy dispersive spectroscopy (EDS) was also used to examine the composition along the coating thickness.

2.3 Antibacterial Behavior

The antibacterial activity of the copper coatings, copper anode, and stainless steel sheets was tested using a standard procedure based on the Japanese JIS Z 2801:2000 spread plate method (Ref 25). Two bacterial species, gram negative *Escherichia coli* NCTC 10418 and gram positive *Staphylococcus aureus* NCTC 11047 were selected as test bacteria. The bacteria were cultured in Tryptone soya agar (Oxoid, UK) overnight and then diluted in Tryptone soya broth (Oxoid, UK) to an optical density OD600 nm of 0.05, which is equivalent to 107 cells/mL. Bacterial suspension with 10^5 cell/mL was prepared. Samples were sterilized by autoclaving, followed by placing on sterile filter papers saturated with distilled water inside sterile 90 mm diameter Petri dishes to maintain ambient humidity. 20 mL of the diluted bacterial suspension were added onto each sample, and the samples were then covered with a sterile glass cover slip in order to maintain the same contact area of suspension on each tested sample surface. All Petri dishes were incubated at room temperature for the designated duration. Times of 60, 120, 240, and 360 min were used to monitor the relation between the percentage of cells killed and contact time (reduction rate).

After the designated time, the sample was transferred to 10 mL of sterile phosphate-buffered saline (PBS) (Sigma) in a sterile container. The contents were vortex mixed for 10 s to dislodge the cover slips and suspend the surviving bacteria in the PBS. Serial dilutions of the bacterial suspension were made and 100 µL aliquots of each dilution was added onto Tryptone soya agar plates, which were incubated overnight at 37 °C. The number of colony forming units (CFU) resulting from the growth of the viable bacterial at 37 °C after 24 h represented the initial viability of the bacteria that survived in the suspension. The percentage reduction was calculated according to the following equation:

$$\text{Reduction } \% \ [(N_0 - N_R)/N_0] \times 100 = (\text{CFU/mL}) \quad \text{(Eq 1)}$$

where N_R is the mean CFU/mL from a test sample after a designated contact time and N_0 is the mean CFU/mL for

the same material sample at time zero. Three specimens of each test material and the controls were analyzed and three plates were spread from the PBS suspension resulting from each sample (Ref 26). The process of desiccation often reduces microbial populations by killing a portion of the cells. The scale of this reduction (from very little to several orders of magnitude) depends on a wide range of factors including strain and culture conditions as well as humidity and temperature during drying. In this research, this phenomenon has been handled by isolation of samples in a sterile shield and reduction of exposure time of bacteria on the surface (Ref 27). Results are expressed as mean ± SD of the measurements.

2.4 Statistical Analysis

All the antibacterial tests were repeated three times. Data were subjected to variance analysis using SAS software (Version 09). Data were pooled for homogenization of the variance. The mean comparisons were calculated in probability level of 1 percentage using least significant difference (LSD) test.

3. Results and Discussion

3.1 Investigation of X-Ray Diffraction Test

The XRD pattern of the copper coatings is shown in Fig. 1. Main phase composition in the XRD pattern is attributed to pure copper (shown with stars). Some minor peaks belonging to copper dioxide (shown with circles) can also be detected. The existence of copper dioxide is due to oxidation of the molten copper particles during spraying by atomizing air and cooling after impact (Ref 28).

3.2 Microstructural Analysis

Microstructure of the commercial copper anode is shown in Fig. 2(a). The average grain size was around 30 μm, which could be defined as a micrograin size structure. The coating microstructure presented in Fig. 2(b) exhibited good interface and adhesion bonding with individual splats locked onto the surface irregularities. The thickness of the copper coating was about 500 μm.

The etched copper coating microstructure is shown in Fig. 3(a) and (b). The columnar structure of grains inside the individual splats indicated the heat transfer direction during solidification. This was perpendicular to the substrate, indicating preferred and columnar-oriented growth within the core region of the splat. Such a microstructure is produced by heterogeneous nucleation of the solid at the interface, followed by growth of the solidification front perpendicular to the interface. The average grain width measured by image analyzer software (Image Tool, IT, 3.0) was around 260 nm. It can be noted that there are some pores in the copper coating, mainly between the splats.

Surface morphology of the copper coating is illustrated in Fig. 4(a) and (b). The diameter of splats was estimated to be around 100 μm. As is common for wire arc spray, most of the sprayed particles were completely molten before colliding with the substrate.

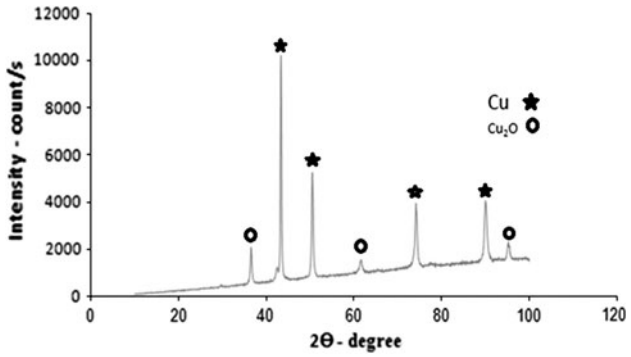

Fig. 1 X-ray diffraction pattern from the surface of the copper coating

3.3 Evaluation of Oxidation During Deposition Process

Thin oxide layers (mainly, copper oxides) were formed between individual splats inside the copper coating as shown in EDS mapping and SEM images (Fig. 5a, b). Analysis shows that decreasing the particle size leads to a higher level of their oxidation. The smaller particles have oxides distributed over the entire volume of the particle whereas with an increase in particle size, the particle develops an oxide coating or shell. Thus, the oxidation of an in-flight particle proceeds from particle surface towards the center (Ref 28, 29). Oxide inclusions outlining the grain or splat boundaries have also been noted (Ref 30). Particles with more surface oxidation were observed in a wire arc sprayed deposit.

As Fig. 6(a) illustrates an EDS line scan through about 14 μm of the cross section of the as-sprayed structure, which consists of five individual splats, verifies the distribution of oxygen in the lamellae boundaries. The coating microstructure in Fig. 6(b) shows splats on top of each other separated by alternating oxide layers. The distinctions between the splat layers are clearly defined. Oxide stringers separate these splat lamellae. A variety of microstructures are observed in the wire arc spray deposit, resulting from variations in the particle trajectories, oxidation behavior, and melting efficiency (Ref 31).

3.4 Antibacterial Susceptibility Evaluation

Reduction in bacterial numbers of *S. aureus* NCTC 11047 and *E. coli* NCTC 10418 after contact with three different surfaces is indicated in Fig. 7(a) and (b), respectively. *E. coli* NCTC 10418 was more sensitive to the inhibitory action of the copper coating (97% after 6 h), whereas *S. aureus* needed a longer time to reach a

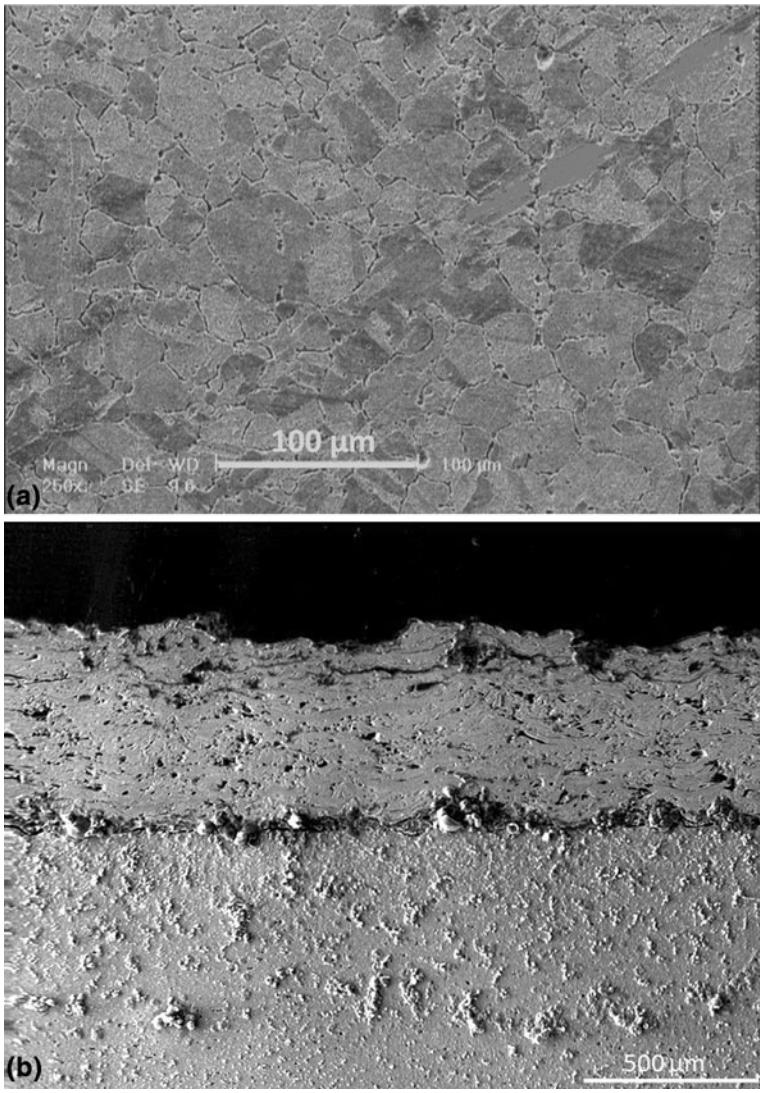

Fig. 2 SEM micrographs from cross section of (a) commercial copper anode and (b) wire arc sprayed copper coating

similar percentage of reduction. Compared to stainless steel, the copper coating exhibited higher antibacterial activity. *E. coli* and *S. aureus* only survived for very short periods of time on the copper coatings. The killing rate for stainless steel was in the range of 8-24 h. In comparison with the copper anode, antibacterial activity of the copper coating was much better, i.e., viable bacteria on the copper coating were killed in a shorter period of time. The mechanism of the copper toxicity to bacteria remains to be fully understood, but it has been reported that it is associated with a bacteria interaction with protein thiol groups. More recently, Lansdown et al. (Ref 26) demonstrated that silver binds to bacterial DNA and RNA and inhibits bacterial replication. The bactericidal effect of copper is caused by the release of Cu ions when metal is in contact with water. Thus, the cell membrane will be damaged or the function of enzymes will be altered when released Cu ions are absorbed on the cell surface. These interactions could explain the non-selective biocidal activity of copper on *E. coli* and *S. aureus*. Defects of the coating structure such as incoherent twin boundaries, micropores and microcracks are energetically favorable as segregation points for solute atoms such as oxygen. More importantly, these sites contribute to differences in energy states on the copper coating and, hence, provide the necessary driving force for sustained dissolution of metal ions from the surface. The physical nature of the copper crystallites, in the form of nanocrystals, and their association with Cu-O super oxides and defects acting as preferential dissolution sites in aqueous media, are crucial to providing enhanced antibacterial activity (Ref 32, 33). However, the attachment and growth of the bacteria on the biomaterial surface depends on various factors, including the morphology and free energy of the surface, the characteristics of the bacteria and the surrounding environment, such as the medium and temperature. In this study bacterial cells and environmental factors were kept constant (Ref 26).

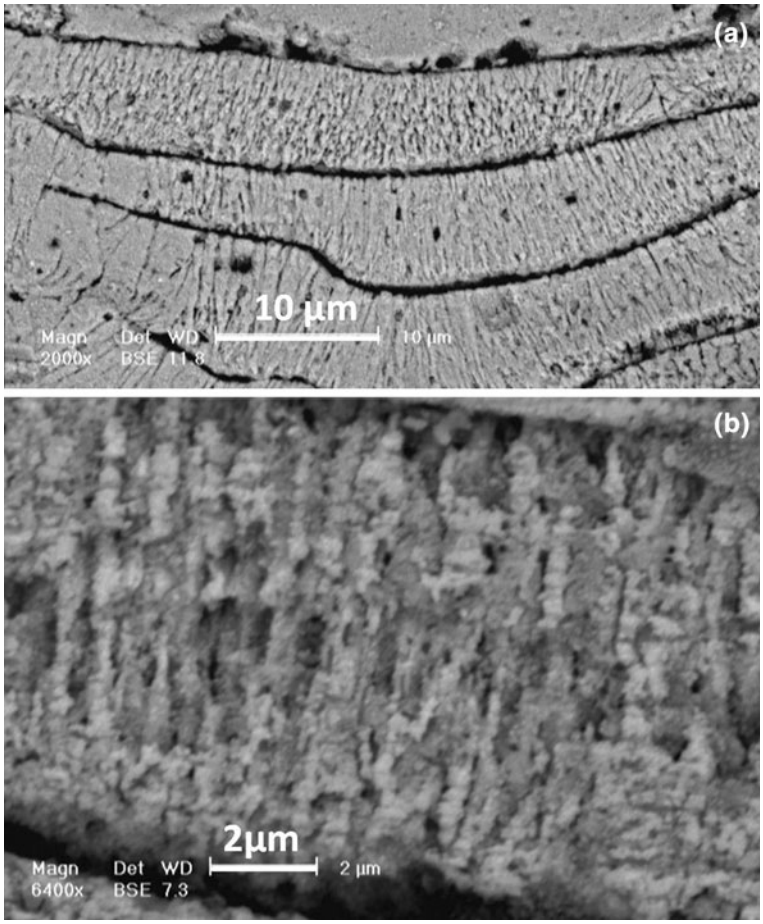

Fig. 3 SEM micrograph of (a) microstructure of splats in copper coating and (b) microstructure of grains in copper coating

3.5 Statistical Analysis

Table 2 shows the variance analysis of the antibacterial data. The results of antibacterial rate treatment (*S. aureus* and *E. coli* bacteria) for all three samples were significant ($p \leq 0.01$). The highest and lowest percentage of bacteria viable was observed in control treatment of stainless steel (66.6%) and copper coating (37.4%), respectively (Table 3). Table 3 shows the statistical analysis of the effect of time and material on antibacterial treatment, which indicated that the time and material treatment interactions were significant for antibacterial rate ($p \leq 0.01$). The highest antibacterial rate was obtained in 360 min for copper coating treatment (6.67%), which had a significant difference with other treatments.

The effect of materials (copper coating, commercially available copper, stainless steel) was significant on antibacterial rate (*S. aureus* bacteria) (Table 2) ($p \leq 0.01$). The maximum percentage of bacteria viable was obtained in the control treatment of stainless steel (68.02%) and the minimum percentage was related to the treatment of copper coating (39.06%) as indicated in Table 3. Hence, the best treatment of time and materials subjected to the best antibacterial behavior was the treatment of copper coating in 360 min (8.07%), which had a significant difference with other treatments.

4. Summary and Conclusion

Copper coatings were successfully deposited on a stainless steel substrate by wire arc spraying for antibacterial applications. The coating microstructure showed splats on top of each other separated by alternating oxide layers. Viable bacteria on the copper coating were killed in a shorter period of time in comparison to copper sheet and stainless steel 316. *E. coli* NCTC 10418 was more sensitive to the biocidal action of the copper coating (97% after 6 h), whereas *S. aureus* needed longer time to reach a similar percentage of reduction. In summary, the results presented in this paper suggest that the bactericide properties of the twin wire arc sprayed copper coating could be a function of the coating grain size, defects such as micropores, microcracks, and specific oxygen species. Statistical analysis showed that the antibacterial properties of the copper coatings were significantly better than other samples.

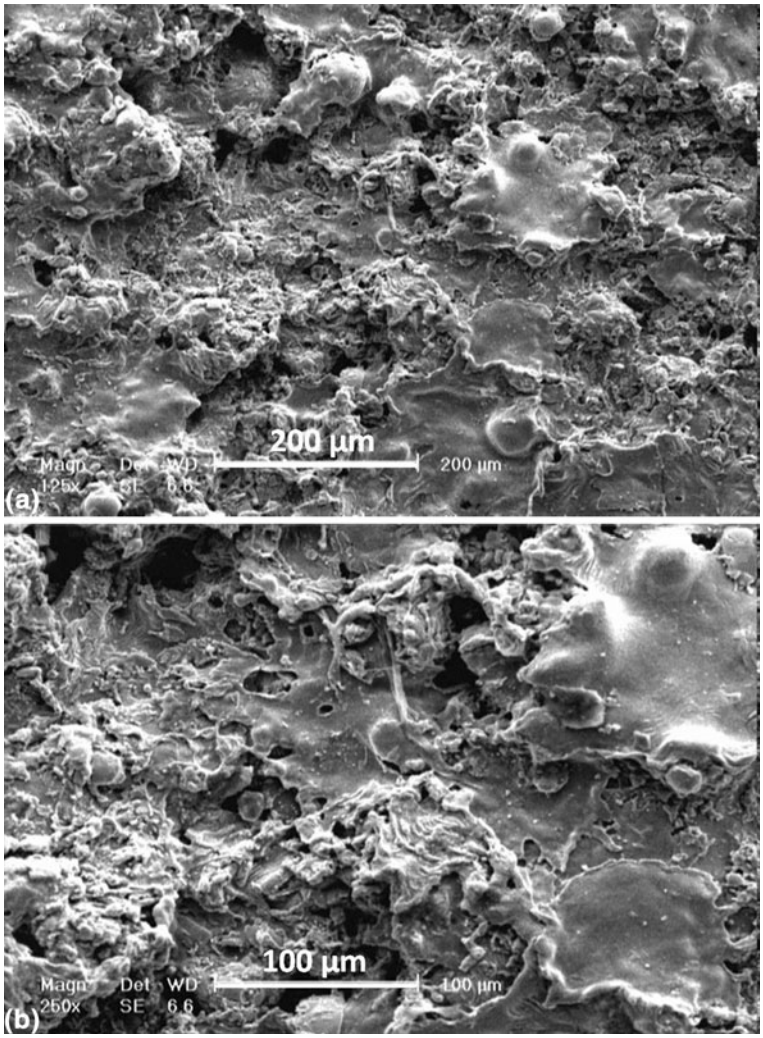

Fig. 4 SEM micrographs from the surface morphology of copper coating with two different magnifications: (a) 125×, (b) 500×

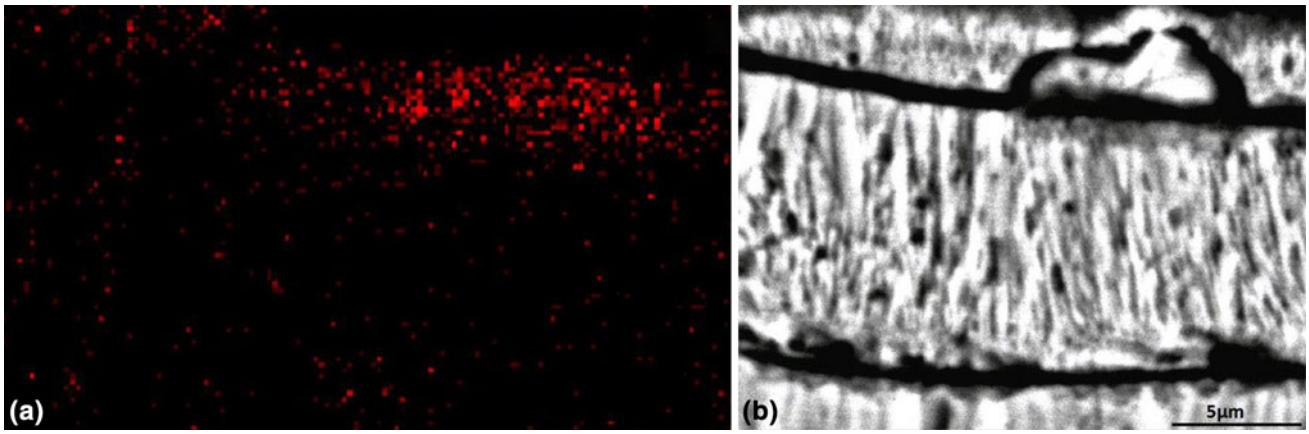

Fig. 5 EDS mapping of the as-sprayed copper coating showing oxide layer: (a) oxygen mapping, (b) SEM image

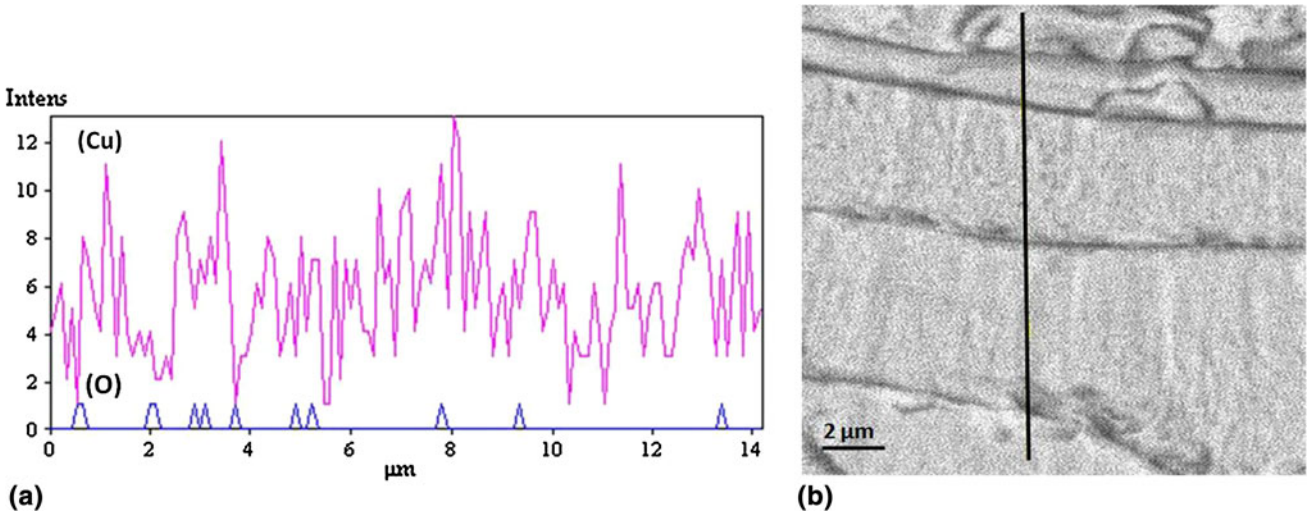

Fig. 6 As-sprayed copper coating: (a) line scan, (b) SEM micrograph of cross section

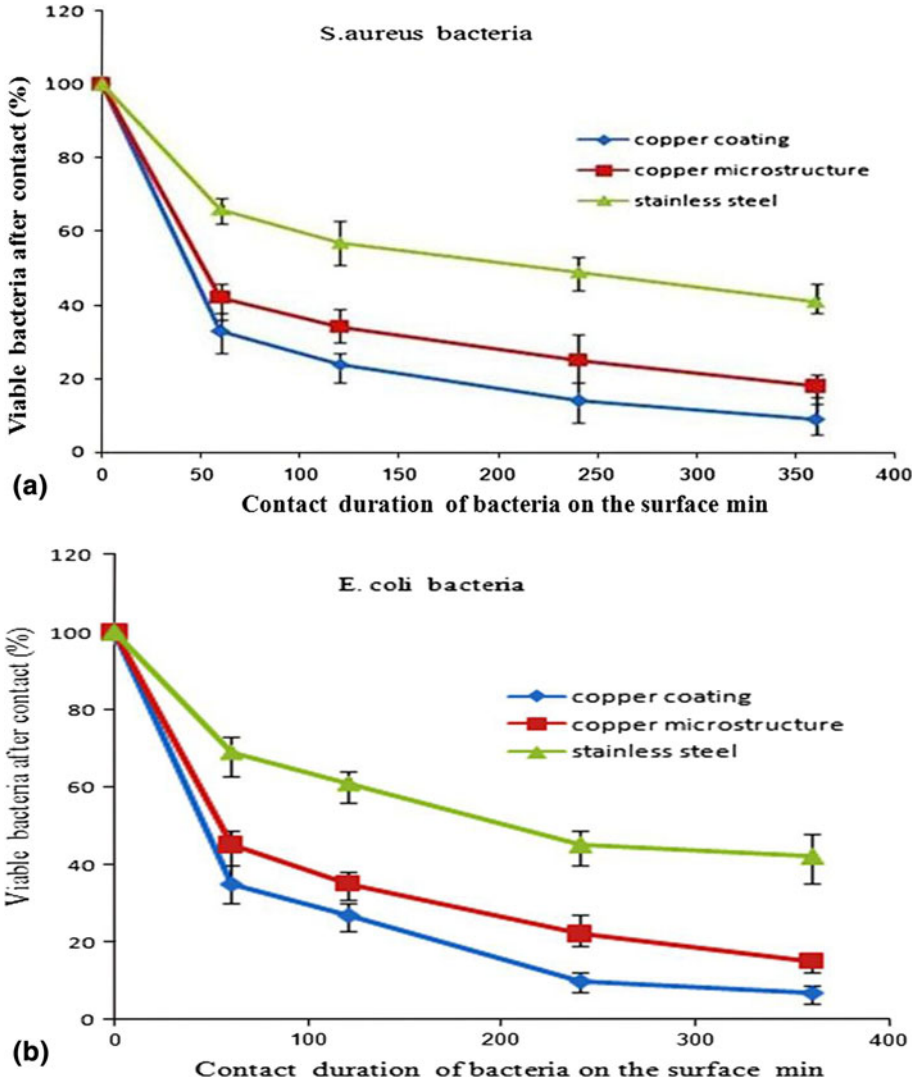

Fig. 7 Reduction in bacterial numbers after contact with the surfaces (a) *S. aureus* NCTC 11047, (b) *E. coli* NCTC 10418

Table 2 Variance analysis of data the antibacterial test

Source	Mean square *E. coli*	Mean square *S. aureus*	Degree of freedom
Model	2855.36*	2741.15*	14
Materials	3345.26*	3345.26*	2
Time	7424.42*	7424.42*	4
Materials × Time	248.48*	248.48*	8
Error	5.88	5.95	30

* indicating significant in probability level of 1%

Table 3 Comparison of treatment average by LSD method

Experimental factor	*E. coli*	*S. aureus*
Materials		
Copper coating	37.40	39.06
Copper cathode	46.66	47.93
Stainless steel 316L	66.60	68.02
LSD	1.87	1.82
Time, min		
0	100.00	100.00
60	51.78	53.66
120	41.56	43.44
240	31.89	33.88
360	25.86	27.66
LSD	2.36	2.34

Acknowledgments

The authors gratefully acknowledge the assistance of S.H. Torabian and M. Zamanipour for their valuable input in helping us to conduct this evaluation.

References

1. C.C. Trapalis, M. Kokkoris, G. Perdikakis, and G. Kordas, Study of Antibacterial Composite Cu/Sio_2 Thin Coatings, *J. Sol-Gel Sci. Technol.*, 2003, **26**, p 1213-1218
2. C. Vuong and M. Otto, Management of Bacterial Complications in Critically Ill Patients Surgical Wound and Catheter-Related Infections, *Microbes Infect.*, 2002, **4**, p 481-489
3. M.J. Pelczar and E.C.S. Chan, *Element of Microbiology*, McGraw Hill, New York, 1981, p 494-507
4. K.S. Chen, Y.A. Ku, C.H. Lee, H.R. Lin, F.H. Lin, and T.M. Chen, Immobilization of Chitosan Gel with Cross-Linking Reagent on PNIPAAm Gel/PP Nonwoven Composites Surface, *Mater. Sci. Eng., A*, 2005, **25**, p 472-478
5. W. Zhang, Y. Luo, H. Wang, S. Pu, and P.K. Chu, Biocompatibility of Silver and Copper Plasma Doped Polyethylene, *Surf. Coat. Technol.*, 2007, **201**, p 8606-8609
6. W. Zhang and P.K. Chu, Enhancement of Antibacterial Properties and Biocompatibility of Polyethylene by Silver and Copper Plasma Immersion Ion Implantation, *Surf. Coat. Technol.*, 2008, **203**, p 909-912
7. M. Kowshik, S. Ashtaputre, and S. Kharrazi, Extracellular Synthesis of Silver Nanoparticles by a Silver-Tolerant Yeast Strain MKY_3, *J. Nanosci. Nanotechnol.*, 2003, **14**, p 95-100
8. E. Jouets and W. Levinson, *Microbiology in Medical*, 5th ed., McGraw-Hill, New York, 2005, p 104-127
9. M. Uchida, The Repair of a Bilateral Cleft Lip Nose: Results in Fifteen Cases After Columella-Lengthening, *Chem. Ind.*, 1995, **46**, p 48
10. O. Akhavan and E. Ghaderi, Self-Accumulated Ag Nanoparticles on Mesoporous TiO_2 Thin Film with High Bactericidal Activities, *Surf. Coat. Technol.*, 2010, **204**, p 3676-3683
11. O. Akhavan and E. Ghaderi, Cu and CuO Nanoparticles Immobilized by Silica Thin Films as Antibacterial Materials and Photocatalysts, *Surf. Coat. Technol.*, 2010, **205**, p 219-223
12. H.T. Michels, J.O. Noyce, and C.W. Keevil, Effects of Temperature and Humidity on the Efficacy of Methicillin-Resistant *Staphylococcus aureus* Challenged Anti-microbial Materials Containing Silver and Copper, *Lett. Appl. Microbiol.*, 2009, **49**, p 191-195
13. N. Duran, P.D. Marcato, O.L. Alves, and G. Souza, Antibacterial Effect of Silver Nanoparticles Produced by Fungal Process on Textile Fabrics and Their Effluent Treatment, *J. Biomed. Nanotechnol.*, 2007, **3**, p 203-208
14. Y.Z. Wana, S. Ramanb, F. Hea, and Y. Huang, Surface Modification of Medical Metals by Ion Implantation of Silver and Copper, *Vacuum*, 2007, **81**, p 1114-1118
15. E. Apen, B.R. Rogers, and J.A. Sellers, X-ray Photoelectron Spectroscopy Characterization of the Oxidation of Electroplated and Sputter Deposited Copper Surfaces, *J. Vac. Sci. Technol.*, 1998, **16**, p 1227-1233
16. M.J. Domek, M.W. LeChevallier, S.C. Cameron, and G.A. McFeters, Evidence for the Role of Copper in the Injury Process of Coliform Bacteria in Drinking Water, *Appl. Environ. Microbiol.*, 1984, **48**, p 289-293
17. N. George, M. Mahon, and A. McDonald, Bactericidal Performance of Flame-Sprayed Nanostructured Titania-Copper Composite Coatings, *J. Therm. Spray Technol.*, 2010, **19**, p 1042-1053
18. B. Jeffery, M. Peppler, R.S. Lima, and A. McDonald, Bactericidal Effects of HVOF-Sprayed Nanostructured TiO_2 on *Pseudomonas aeruginosa*, *J. Therm. Spray Technol.*, 2010, **19**, p 344-349
19. M.F. Brunella, M.V. Diamanti, M.P. Pedeferri, F. di Fonzo, C.S. Casari, and A. Li Bassi, Photocatalytic Behavior of Different Titanium Dioxide Layers, *Thin Solid Films*, 2007, **515**, p 6309-6313
20. L. Brook, P. Evans, H. Foster, M. Pemble, A. Steele, D. Sheel, and H. Yates, Highly Bioactive Silver and Silver/Titania Composite Films Grown by Chemical Vapour Deposition, *J. Photochem. Photobiol. A*, 2007, **187**, p 53-63
21. M.P. Planche, H. Liao, and C. Coddet, Relationships Between In-Flight Particle Characteristics and Coating Microstructure with a Twin Wire Arc Spray Process and Different Working Conditions, *Surf. Coat. Technol.*, 2004, **182**, p 215-226
22. S.A. Wilks, H. Michels, and C.W. Keevil, The Survival of *Escherichia coli* O157 on a Range of Metal Surfaces, *Int. J. Food Microbiol.*, 2005, **105**, p 445-454
23. J.O. Noyce, H. Michels, and C.W. Keevil, Inactivation of Influenza A Virus on Copper Versus Stainless Steel Surfaces, *Appl. Environ. Microbiol*, 2007, **73**, p 2748-2750
24. T. Stoltenhoff, C. Borchers, F. Gartner, and H. Kreye, Microstructures and Key Properties of Cold-Sprayed and Thermally Sprayed Copper Coatings, *Surf. Coat. Technol.*, 2006, **200**, p 4947-4960
25. S. Suzuki, S. Imai, and H. Kourai, Background and Evidence Leading to the Establishment of the JIS Standard for Antimicrobial Products, *Biocontrol Sci.*, 2006, **11**(3), p 135-145
26. Y. Dong, X. Li, L. Tian, T. Bell, R.L. Sammons, and H. Dong, Towards Long-Lasting Antibacterial Stainless Steel Surfaces by Combining Double Glow Plasma Silvering with Active Screen Plasma Nitriding, *Acta Biomater.*, 2011, **7**, p 447-457

27. M. Potfis, Desiccation Tolerance of Prokaryotes, *Microbiol. Rev.*, 1994, **58**, p 755-805
28. S. Deshpande, S. Sampath, and H. Zhang, Mechanisms of Oxidation and Its Role in Microstructural Evolution of Metallic Thermal Spray Coatings-Case Study for Ni-Al, *Surf. Coat. Technol.*, 2006, **200**, p 5395-5406
29. S. Sampath and H. Herman, Rapid Solidification and Microstructure Development During Plasma Spray Deposition, *J. Therm. Spray Technol.*, 1996, **5**, p 445-448
30. C.J. Li and B. Sun, Microstructure and Property of Micro-Plasma-Sprayed Cu Coating, *Mater. Sci. Eng., A*, 2004, **379**, p 92-101
31. F. Wu, E.H. Jordan, X. Ma, and M. Gell, Thermally Grown Oxide Growth Behavior and Spallation Lives of Solution Precursor Plasma Spray Thermal Barrier Coatings, *Surf. Coat. Technol.*, 2008, **202**, p 1628-1635
32. S.B. Santa, K.S. Gill, and R.E. Burrell, Nanostructure, Dissolution and Morphology Characteristics of Microcidal Silver Films Deposited by Magnetron Sputtering, *Acta Biomater.*, 2007, **3**, p 341-350
33. W. Shao and Q. Zhao, Influence of Reducers on Nanostructure and Surface Energy of Silver Coatings and Bacterial Adhesion, *Surf. Coat. Technol.*, 2010, **204**, p 1288-1294